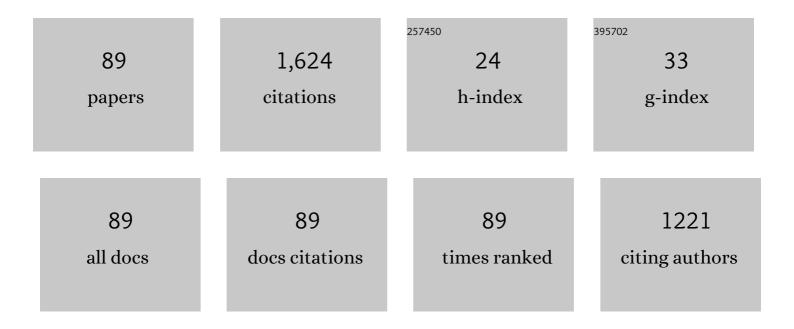
Yingjie Zhang

List of Publications by Year in descending order

Source: https://exaly.com/author-pdf/632309/publications.pdf Version: 2024-02-01



#	Article	IF	CITATIONS
1	Twisted Cucurbit[<i>n</i>]urils. Organic Letters, 2016, 18, 4020-4023.	4.6	120
2	Crystal chemistry and structures of uranium-doped gadolinium zirconates. Journal of Nuclear Materials, 2013, 438, 144-153.	2.7	50
3	The incorporation of plutonium in lanthanum zirconate pyrochlore. Journal of Nuclear Materials, 2013, 443, 444-451.	2.7	44
4	Specific recognition of formaldehyde by a cucurbit[10]uril-based porous supramolecular assembly incorporating adsorbed 1,8-diaminonaphthalene. Journal of Materials Chemistry C, 2019, 7, 1597-1603.	5.5	39
5	Pyrochlore-structured titanate ceramics for immobilisation of actinides: Hot isostatic pressing (HIPing) and stainless steel/waste form interactions. Journal of Nuclear Materials, 2008, 377, 470-475.	2.7	38
6	Development of brannerite glassâ€ceramics for the immobilization of actinideâ€rich radioactive wastes. Journal of the American Ceramic Society, 2017, 100, 4341-4351.	3.8	38
7	Uranium(<scp>vi</scp>) complexes with isonicotinic acid: from monomer to 2D polymer with unique U–N bonding. RSC Advances, 2015, 5, 33249-33253.	3.6	37
8	Hot isostatically pressed Y2Ti2O7 and Gd2Ti2O7 pyrochlore glass-ceramics as potential waste forms for actinide immobilization. Journal of the European Ceramic Society, 2019, 39, 1546-1554.	5.7	37
9	Crystal Chemistry and Structures of (Ca,U) Titanate Pyrochlores. Journal of the American Ceramic Society, 2010, 93, 3464-3473.	3.8	35
10	Zirconolite glass-ceramics for plutonium immobilization: The effects of processing redox conditions on charge compensation and durability. Journal of Nuclear Materials, 2017, 490, 238-241.	2.7	35
11	Preparation of Y2Ti2O7 pyrochlore glass-ceramics as potential waste forms for actinides: The effects of processing conditions. Journal of Nuclear Materials, 2017, 494, 29-36.	2.7	35
12	Plutonium in monazite and brabantite: Diffuse reflectance spectroscopy study. Journal of Nuclear Materials, 2008, 375, 311-314.	2.7	32
13	Current advances on titanate glass-ceramic composite materials as waste forms for actinide immobilization: A technical review. Journal of the European Ceramic Society, 2022, 42, 1852-1876.	5.7	32
14	Raman spectroscopic study of natural and synthetic brannerite. Journal of Nuclear Materials, 2013, 437, 149-153.	2.7	31
15	Uranium brannerite with Tb(III)/Dy(III) ions: Phase formation, structures, and crystallizations in glass. Journal of the American Ceramic Society, 2019, 102, 7699-7709.	3.8	31
16	Uranium(VI) coordination polymers with pyromellitate ligand: Unique 1D channel structures and diverse fluorescence. Journal of Solid State Chemistry, 2015, 226, 42-49.	2.9	30
17	Synthesis, characterisation and influence of lipophilicity on cellular accumulation and cytotoxicity of unconventional platinum(<scp>iv</scp>) prodrugs as potent anticancer agents. Dalton Transactions, 2019, 48, 17228-17240.	3.3	30
18	Water Molecule-Induced Reversible Magnetic Switching in a Bis-Terpyridine Cobalt(II) Complex Exhibiting Coexistence of Spin Crossover and Orbital Transition Behaviors. Inorganic Chemistry, 2020, 59, 16843-16852.	4.0	30

#	Article	IF	CITATIONS
19	Synthesis and characterisation of uranyl substituted malonato complexes. Polyhedron, 2002, 21, 69-79.	2.2	28
20	Synthesis and Analysis of the Structure, Diffusion and Cytotoxicity of Heterocyclic Platinum(IV) Complexes. Chemistry - A European Journal, 2015, 21, 16990-17001.	3.3	28
21	Structural and spectroscopic investigations on the crystallization of uranium brannerite phases in glass. Journal of the American Ceramic Society, 2018, 101, 5219-5228.	3.8	28
22	Dysprosium complexes with mono-/di-carboxylate ligands—From simple dimers to 2D and 3D frameworks. Journal of Solid State Chemistry, 2014, 219, 1-8.	2.9	27
23	Cytotoxicity and Structural Analyses of 2,2′â€Bipyridineâ€, 4,4′â€Dimethylâ€2,2′â€bipyrÂidine―and 2â€(2′â€Pyridyl)quinoxalineplatinum(II) Complexes. European Journal of Inorganic Chemistry, 2015, 2015, 4167-4175.	2.0	27
24	A new method for production of glass-Ln2Ti2O7 pyrochlore (Ln = Gd, Tb, Er, Yb). Journal of the European Ceramic Society, 2017, 37, 4963-4972.	5.7	27
25	Phase evolution from Ln ₂ Ti ₂ O ₇ (Ln=Y and Gd) pyrochlores to brannerites in glass with uranium incorporation. Journal of the American Ceramic Society, 2017, 100, 5335-5346.	3.8	26
26	Self-assembly of a unique 3d/4f heterometallic square prismatic box-like coordination cage. Dalton Transactions, 2016, 45, 9407-9411.	3.3	25
27	CO ₂ â€Induced Spinâ€&tate Switching at Room Temperature in a Monomeric Cobalt(II) Complex with the Porous Nature. Angewandte Chemie - International Edition, 2020, 59, 10658-10665.	13.8	25
28	Solvothermal synthesis of uranium(VI) phases with aromatic carboxylate ligands: A dinuclear complex with 4-hydroxybenzoic acid and a 3D framework with terephthalic acid. Journal of Solid State Chemistry, 2016, 234, 22-28.	2.9	24
29	Synthesis and characterisation of uranyl substituted malonato complexes. Polyhedron, 2002, 21, 81-96.	2.2	23
30	Investigating the cytotoxicity of platinum(II) complexes incorporating bidentate pyridyl-1,2,3-triazole "click―ligands. Journal of Inorganic Biochemistry, 2016, 165, 92-99.	3.5	22
31	Hydrothermal synthesis, structures and properties of two uranyl oxide hydroxyl hydrate phases with Co(<scp>ii</scp>) or Ni(<scp>ii</scp>) ions. New Journal of Chemistry, 2016, 40, 5357-5363.	2.8	22
32	Pyrochlore glassâ€eeramics fabricated via both sintering and hot isostatic pressing for minor actinide immobilization. Journal of the American Ceramic Society, 2020, 103, 5470-5479.	3.8	22
33	Theoretical and experimental Raman spectroscopic studies of synthetic thorutite (ThTi2O6). Journal of Nuclear Materials, 2014, 446, 68-72.	2.7	19
34	Dioxo-vanadium(<scp>v</scp>), oxo-rhenium(<scp>v</scp>) and dioxo-uranium(<scp>vi</scp>) complexes with a tridentate Schiff base ligand. RSC Advances, 2016, 6, 75045-75053.	3.6	19
35	Uranium(VI) hybrid materials with [(UO ₂) ₃ (µ ₃ â€O)(µ ₂ â€OH) ₃] ⁺ the sub–building unit via uranyl–cation interactions. ChemistrySelect, 2016, 1, 7-12.	ası.5	19
36	Phase evolution and microstructure analysis of CaZrTi2O7 zirconolite in glass. Ceramics International, 2018, 44, 6285-6292.	4.8	19

#	Article	IF	CITATIONS
37	Synthesis and crystal structures of uranium (VI) and thorium (IV) complexes with picolinamide and malonamide. Inorganic Chemistry Communication, 2013, 37, 219-221.	3.9	18
38	Uranyl oxide hydrate phases with heavy lanthanide ions: [Ln(UO ₂) ₂ O ₃ (OH)]·0.5H ₂ O (Ln = Tb, Dy, Ho and Yb). New Journal of Chemistry, 2018, 42, 12386-12393.	2.8	18
39	Syntheses, Crystal Structures, and Spectroscopic Studies of Uranyl Oxide Hydrate Phases with La(III)/Nd(III) Ions. Inorganic Chemistry, 2019, 58, 10812-10821.	4.0	18
40	Kinetics vs. thermodynamics: a unique crystal transformation from a uranyl peroxo-nanocluster to a nanoclustered uranyl polyborate. RSC Advances, 2014, 4, 34244-34247.	3.6	17
41	Syntheses, structures and magnetic properties of tetranuclear cubane-type and heptanuclear wheel-type nickel(<scp>ii</scp>) complexes with 3-methoxysalicylic acid derivatives. Dalton Transactions, 2017, 46, 8555-8561.	3.3	17
42	Comparison of uranium(VI) and thorium(IV) coordination polymers with p-toluenesulfonic acid. Polyhedron, 2015, 91, 98-103.	2.2	16
43	Synthesis, characterisation and potent cytotoxicity of unconventional platinum(<scp>iv</scp>) complexes with modified lipophilicity. Dalton Transactions, 2019, 48, 17217-17227.	3.3	16
44	The incorporation of neptunium and plutonium in thorutite (ThTi2O6). Journal of Alloys and Compounds, 2013, 581, 665-670.	5.5	14
45	High-Pressure Synthesis, Structural, and Spectroscopic Studies of the Ni–U–O System. Inorganic Chemistry, 2018, 57, 13847-13858.	4.0	14
46	Spectroscopic Studies and Crystal Structures of Double Thorium(IV) Oxalates with Sodium Ions. European Journal of Inorganic Chemistry, 2013, 2013, 6170-6174.	2.0	13
47	Synthesis, spectroscopic characterization and crystal structures of thorium(IV) mononuclear lactato and hexanuclear formato complexes. Polyhedron, 2015, 87, 377-382.	2.2	13
48	Neodymium coordination polymers with propionate, succinate and mixed succinate–oxalate ligands: Synthesis, structures and spectroscopic characterization. Polyhedron, 2015, 102, 130-136.	2.2	13
49	CaZrTi ₂ O ₇ zirconolite synthesis: From ceramic to glassâ€ceramic. International Journal of Applied Ceramic Technology, 2019, 16, 1460-1470.	2.1	12
50	[U(H ₂ 0) ₂]{[(UO ₂) ₁₀ O ₁₀ (OH) _{2A Mixed-Valence Uranium Oxide Hydrate Framework. Inorganic Chemistry, 2020, 59, 12166-12175.}	>][(UO <su< td=""><td>b>4)(H</td></su<>	b>4)(H
51	The incorporation of Nd or Ce in CaZrTi2O7 zirconolite: Ceramic versus glass-ceramic. Journal of Nuclear Materials, 2021, 543, 152583.	2.7	12
52	Pyrochlore glass-ceramics for the immobilization of molybdenum-99 production wastes: Demonstrating scalability and flexibility to waste stream variance. Journal of the European Ceramic Society, 2021, 41, 7269-7281.	5.7	12
53	Layer-structured uranyl-oxide hydroxy-hydrates with Pr(<scp>iii</scp>) and Tb(<scp>iii</scp>) ions: hydroxyl to oxo transition driven by interlayer cations. Dalton Transactions, 2020, 49, 5832-5841.	3.3	11
54	Diffuse reflectance spectroscopy of tetravalent neptunium and plutonium ions in ThO2. Journal of Nuclear Materials, 2008, 374, 192-196.	2.7	10

#	Article	IF	CITATIONS
55	Thorium(IV) organic frameworks with aromatic polycarboxylate ligands. Journal of Inclusion Phenomena and Macrocyclic Chemistry, 2015, 82, 163-172.	1.6	10
56	3d transition metal complexes with a julolidine–quinoline based ligand: structures, spectroscopy and optical properties. Inorganic Chemistry Frontiers, 2016, 3, 286-295.	6.0	10
57	Uranyl oxide hydrate frameworks with lanthanide ions. Dalton Transactions, 2020, 49, 15854-15863.	3.3	10
58	Synthetic uranium oxide hydrate materials: Current advances and future perspectives. Dalton Transactions, 2022, , .	3.3	10
59	Uranyl peroxide clusters stabilized by dicarboxylate ligands: A pentagonal ring and a dimer with extensive uranyl–cation interactions. Polyhedron, 2015, 92, 99-104.	2.2	9
60	Surface evolution and radiation damage of a zirconolite glass-ceramic by Au ion implantation. Applied Surface Science, 2019, 478, 373-382.	6.1	9
61	Lanthanoid Heteroleptic Complexes with Cucurbit[5]uril and Dicarboxylate Ligands: From Discrete Structures to One-Dimensional and Two-Dimensional Polymers. Inorganic Chemistry, 2019, 58, 506-515.	4.0	9
62	Hydrothermal Syntheses of Uranium Oxide Hydrate Materials with Sm(III) Ions: pH-Driven Diversities in Structures and Morphologies and Sm-Doped Porous Uranium Oxides Derived from Their Thermal Decompositions. Inorganic Chemistry, 2021, 60, 13233-13241.	4.0	9
63	Phase assemblage and microstructures of Gd2Ti2-xZrxO7 (x = 0.1–0.3) pyrochlore glass-ceramics as potential waste forms for actinide immobilization. Materials Chemistry and Physics, 2021, 273, 125058.	4.0	9
64	Sodium zirconium phosphateâ€based glassâ€ceramics as potential wasteforms for the immobilization of nuclear wastes. Journal of the American Ceramic Society, 2022, 105, 901-912.	3.8	9
65	HIPed Tailored Pyrochlore-Rich Glass-Ceramic Waste Forms for the Immobilization of Nuclear Waste. Materials Research Society Symposia Proceedings, 2008, 1124, 1.	0.1	8
66	One-dimensional uranium(VI) coordination polymers with pyridinecarboxylate ligands. Polyhedron, 2016, 113, 88-95.	2.2	8
67	Syntheses and crystal structures of thorium(IV) and uranium(IV) tripodal metalloligands. Polyhedron, 2017, 138, 82-87.	2.2	8
68	Thorium(IV) and Uranium(IV) Complexes with Cucurbit[5]uril. Inorganic Chemistry, 2018, 57, 8588-8598.	4.0	8
69	Thorium(<scp>iv</scp>) and uranium(<scp>vi</scp>) compounds of cucurbit[10]uril: from a one-dimensional nanotube to a supramolecular framework. Dalton Transactions, 2020, 49, 404-410.	3.3	8
70	Diffuse reflectance spectroscopy of neptunium ions in polycrystalline ceramics designed for immobilization of HLW. Journal of Alloys and Compounds, 2007, 444-445, 598-602.	5.5	7
71	New synthesis route for lead zirconate titanate powder. Ceramics International, 2016, 42, 6782-6790.	4.8	6
72	Combining the platinum(ii) drug candidate kiteplatin with 1,10-phenanthroline analogues. Dalton Transactions, 2018, 47, 2156-2163.	3.3	6

#	Article	IF	CITATIONS
73	Creating capsules with cubanes. Dalton Transactions, 2018, 47, 9575-9578.	3.3	6
74	Magnetism in a helicate complexes arising with the tetradentate ligand. Dalton Transactions, 2021, 50, 494-498.	3.3	6
75	Hot isostatic pressed pyrochlore glass eramics: Revealing structure insides at the reaction interface. Journal of the American Ceramic Society, 2021, 104, 5981-5989.	3.8	6
76	An investigation of LnUO4 (Ln = Dy and Ho): Structures, microstructures, uranium valences and magnetic properties. Journal of the European Ceramic Society, 2021, 41, 6000-6009.	5.7	6
77	Synthesis and characterization of a uranium oxide hydrate framework with Sr(<scp>ii</scp>) ions: structural insights and mixed uranium valences. New Journal of Chemistry, 2022, 46, 1371-1380.	2.8	6
78	Profiling hot isostatically pressed canister–wasteform interaction for Puâ€bearing zirconoliteâ€rich wasteforms. Journal of the American Ceramic Society, 2022, 105, 5359-5372.	3.8	5
79	Cu(II) ion directed self-assembly of a Y8/Cu6 heterometallic coordination cage via an Y(III) metalloligand. Inorganica Chimica Acta, 2019, 484, 521-526.	2.4	4
80	CO 2 â€Induced Spinâ€6tate Switching at Room Temperature in a Monomeric Cobalt(II) Complex with the Porous Nature. Angewandte Chemie, 2020, 132, 10745-10752.	2.0	4
81	Ceramic Waste Forms. , 2020, , 445-466.		4
82	Dinuclear complexes of europium(III) and gadolinium(III) ions with a julolidine–quinoline-based tridentate ligand. Journal of Coordination Chemistry, 2016, 69, 1883-1892.	2.2	3
83	Hydrothermal synthesis, structures and magnetic properties of two new holmium(III) oxalato complexes. Journal of Coordination Chemistry, 2017, 70, 2040-2051.	2.2	3
84	Yttrium and lanthanide (Ln = La and Gd) complexes with cucurbit[10]uril: crystals transforming from supramolecular frameworks to coordination nanotubes. New Journal of Chemistry, 2020, 44, 18208-18215.	2.8	3
85	Syntheses and crystal structures of two uranyl peroxide nanoclusters with a diphosphonate linker ligand. Polyhedron, 2019, 174, 114161.	2.2	2
86	Thorium(IV) and uranium(IV) complexes with cucurbit[8]uril: Supramolecular structures via direct coordination and second-shell interactions. Polyhedron, 2020, 192, 114826.	2.2	2
87	Lanthanide mononuclear complexes with a tridentate Schiff base ligand: Structures, spectroscopies and properties. Polyhedron, 2019, 165, 125-131.	2.2	1
88	The Structural Characterization of a Series of Uranium-containing Gadolinium Zirconates. Materials Research Society Symposia Proceedings, 2012, 1475, 179.	0.1	0
89	Structure Insides at the Reaction Interface Between Pyrochlore Glass-Ceramics and Stainless Steel Canister Under Hot Isostatic Pressing Conditions. SSRN Electronic Journal, 0, , .	0.4	0